

Oblique propagations of ion waves near the ion cyclotron frequency

Toshiro Ohnuma, Tsuneo Kuwabara, Saburo Adachi, and Kan Shibata

Department of Electrical Engineering, Tohoku University, Sendai, Japan

(Received 14 June 1976)

For an excitation by a small probe in a magnetized plasma, we observed ray velocities (phase velocities in the direction of group velocities) of ion waves near the ion cyclotron frequency. The propagation of ion waves from the exciter was found to be restricted inside a fixed cone angle which corresponds to a low-frequency resonance cone.

I. INTRODUCTION

Electrostatic ion waves in a magnetic field have been theoretically investigated by Stepanov and co-workers,^{1,3} Stix,² and others. For an infinite highly non-isothermal ($T_e \gg T_i$) plasma, the existence of two modes have been investigated above and below the ion cyclotron frequency. For the mode below the ion cyclotron frequency, the propagation of ion waves is modified by the magnetic field. The mode above the ion cyclotron frequency results from the coupling of the ion acoustic waves and the ion cyclotron motion and is usually referred to as the electrostatic ion cyclotron wave. Kinetic theory had allowed for ion Bernstein modes⁴ above the ion cyclotron frequency. Furthermore, kinetic theory had indicated the coexistence of the electrostatic ion cyclotron wave and the ion acoustic wave.⁵ Experimentally, the effect of the ion cyclotron frequency on the propagations in a magnetic field has been observed⁶ and the coupling of the electrostatic ion cyclotron wave and ion acoustic wave was also observed.⁵ Ion Bernstein waves were also observed.⁴

In this paper, we investigate oblique propagations of ion waves launched by a small probe, especially those below the ion cyclotron frequency. This excitation in a magnetic field means importantly that the launched waves are not plane waves but special wave fronts, and that the angles of wave propagation are not the same as the detection angle in the radial direction. Hence, the main subjects to be investigated are the wave fronts and ray velocities of the ion waves launched by a small probe in a magnetic field.

In Sec. II, the theoretical background is briefly summarized. The experimental setup and experimental results are described in Sec. III. In Sec. IV, the experimental results are compared with the theoretical results, and the relation of those results to the low-frequency resonance cone is discussed. The paper ends with concluding remarks in Sec. V.

II. THEORETICAL BACKGROUND

For an excitation by a small probe, in which an oscillating point charge is expressed as $qe^{-i\omega t}\delta(\vec{r})$, we may formulate the potential $\phi(\vec{r})$ in a magnetized plasma as follows:

$$\phi(\vec{r}) = \frac{\rho e^{-i\omega t}}{2\pi^2} \int_{-\infty}^{\infty} d\vec{k} \frac{e^{i\vec{k}\cdot\vec{r}}}{k^2 D(\vec{k})}, \quad (1)$$

where \vec{k} denotes the wave-number vector. The dielectric constant $D(\vec{k})$ for a magnetized plasma is given by³

$$D(\vec{k}) = 1 + \sum_{j=e,i} \sum_{n=-\infty}^{\infty} \frac{k_{Dj}^2}{k^2} e^{-\lambda} \text{In}(\lambda) [1 + \alpha_{oj} Z(\alpha_n)], \quad (2)$$

$$k_{Dj}^2 \equiv \frac{\omega_{pj}^2}{\kappa T_j / m_j}, \quad \lambda \equiv \frac{k_{\perp}^2 \kappa T_j / m_j}{\omega_{cj}^2},$$

$$\alpha_{nj} \equiv \frac{\omega + n\omega_{cj}}{k_{\parallel} (2\kappa T_j / m_j)^{1/2}},$$

where ω_{pj} , ω_{cj} , T_j , m_j , $Z(\alpha)$, and $\text{In}(\lambda)$ denote the plasma frequency, the cyclotron frequency, the temperature, the mass of the j th component, the plasma dispersion function,⁸ and the modified Bessel function, respectively. The dispersion relation for the magnetized plasma is given by $D(\vec{k})=0$. For an approximation of a fluid model, the dispersion relation is given by

$$\omega^2 = \frac{k_{\parallel}^2 C_s^2}{1 + k^2 / k_{De}^2} + \frac{1}{1 - \omega_{ci}^2 / \omega^2} \frac{k_{\perp}^2 C_s^2}{1 + k^2 / k_{De}^2}, \quad (3)$$

where C_s and k_{De} indicate the ion sound velocity and the electron Debye wave number, respectively. When the wave excitation by a point source expressed by Eq. (1) is considered in an anisotropic medium, it is very fruitful to investigate the phase, group and ray velocities which can be determined from the dispersion relation (or the dielectric constant).

The ray velocity is defined as the phase velocity in the direction of the group velocity. In such an

anisotropic medium as the magnetized plasma, the direction of the group velocity is generally different from that of the phase velocity, i.e., the direction of propagating waves. The directions of the phase and group velocities satisfy the following relation²:

$$\tan \alpha = -\frac{1}{n} \frac{\partial n}{\partial \theta}, \quad (4)$$

where $n (=ck/\omega)$, θ , and α indicate the refractive index, the direction of the phase velocity or the wave normal, and the angle between the directions of the phase and group velocities, respectively. By using the angle α , the phase velocity in the direction of the group velocity, i.e., the ray velocity V_r , is given by

$$V_r = \frac{1}{\cos \alpha} \frac{\omega}{k}, \quad (5)$$

as is known from the definition. It is an important fact that the ray velocity relates directly to the wave fronts which are determined from Eq. (1). The magnitude of the group velocity $V_g = \partial \omega / \partial \mathbf{k}$ is given by

$$V_g = \frac{1}{\cos \alpha} \frac{\partial \omega}{\partial k}. \quad (6)$$

Equations (4)–(6) are very useful relations in anisotropic media, and relation (5) in particular will be used for an explanation of the experimental results in the present work.

For ion waves in a magnetic field, typical phase, group, and ray velocities are indicated in a polar diagram in Fig. 1, which was obtained from the dispersion relation, Eq. (3), of the fluid model. Those velocities are normalized by the ion acoustic velocity $C_s = (\kappa T_e / m_i)^{1/2}$. The marks A–D on the phase-velocity surface correspond to those on the group- and ray-velocity surfaces. In those calculations, relation (4) played a very important role. In Fig. 1, the relations among the phase, group, and ray velocities are clearly indicated. For example, the ray and group velocities which are observed in the direction of V_g (see point C) result from the propagating waves at point C on the phase-velocity surface. Furthermore, the cone angle inside which the phase-velocity surface exists is clearly shown to be different from the cone angle inside which the group-velocity surface exists. When the detection of the wave signals launched by a small probe is considered in the radial direction with respect to the exciter, the information obtained from the detector relates directly to the signals in the direction of the group velocity V_g , i.e., in the direction of $\theta_d = \theta - \alpha$. The direction of the group velocity θ_d which corresponds to that of the flow of wave energy for weak damping

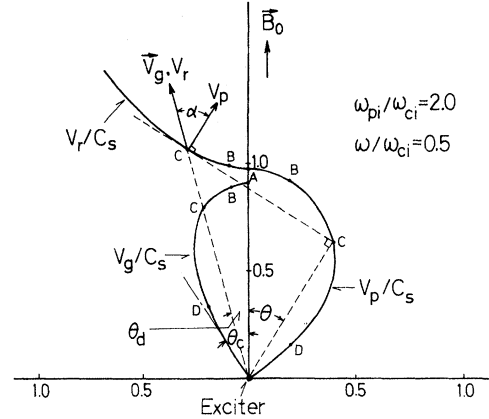


FIG. 1. Typical phase velocity V_p , group velocity V_g , and ray velocity V_r of ion waves in a magnetic field versus the angle to the magnetic field. These are derived from a fluid model and are normalized by an ion acoustic velocity C_s . The marks A–D on the phase-velocity surface correspond to those on the group- and ray-velocity surfaces. The low-frequency resonance cone [Eq. (7)] refers to the angle θ_c . Only one quarter of these surfaces are indicated.

rates is different from the direction of the wave propagation θ . That is, for point-source excitation in anisotropic media, the ray-velocity surface is observed instead of the phase-velocity surface.

III. EXPERIMENTS

A. Experimental setup

The experiments were performed in a vacuum chamber 32 cm in diameter and 160 cm long. The schematic experimental setup is shown in Fig. 2. Helium gas was used at a pressure $P \approx 7 \times 10^{-4}$ Torr. An oxide-coated cathode 10 cm in diameter was set at one side of the chamber for production of forward-diffusing plasmas, in which a grid was used as an anode. Typical plasma parameter values are $N_0 \approx (1-3) \times 10^{18} \text{ cm}^{-3}$ for the plasma den-

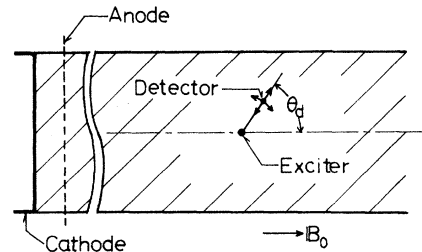


FIG. 2. Schematic experimental setup. The plasma column is 10 cm in diameter. The exciter and the detector are both 1 mm in diameter, and 5 and 3 mm long, respectively. The detector is movable radially and azimuthally.

sity, $T_e = 2-5$ eV for the electron temperature, and $T_i = 0.1-0.3$ eV for the ion temperature. The applied magnetic field was 0.5–1.4 kG. The corresponding ion Larmor radius ranges from $r_L \approx 0.2$ to 0.8 mm. The applied frequency was varied from 100 to 400 kHz. The excitation of the plasma waves was performed with a small probe 1 mm in diameter and 5 mm long. The signals were detected mainly by an interferometer technique with a probe 1 mm in diameter and 3 mm long. The detector was movable radially and azimuthally with respect to the exciter, as shown in the figure.

B. Experimental results

A sinusoidal signal was applied to the exciter; the typical patterns of ion waves in a magnetized plasma are shown in Fig. 3. Those patterns were obtained in the radial direction at several fixed angles. The angle $\theta_d = 0^\circ$ corresponds to the direction of the applied magnetic field. Wave propagations along the magnetic field correspond to those in a nonmagnetized plasma. The observed phase velocity for $\theta = 0^\circ$, $\sim 8 \times 10^5$ cm/sec, is nearly in accord with the ion acoustic velocity. In those experiments of wave propagations, the external voltage applied to the exciter was below 3 V (peak to peak). Under this voltage, the plasma wave behaves linearly in the present experiments because $n/N_0 \approx (2-3)\%$. When the detection angle is not zero ($\theta_d \neq 0$), the waves which propagate obliquely to the magnetic field can be observed. The detected wavelength for $\theta = 10^\circ$ is shown to be larger than that for $\theta = 0^\circ$. That is, the phase velocity for $\theta = 10^\circ$ is faster than that for $\theta = 0^\circ$. As is known from the figure, the observed phase velocity increases with detection angle θ_d . Furthermore, the wave signals were restricted inside a fixed cone angle which will be described in detail below.

In Fig. 4, typical wave fronts, which were ob-

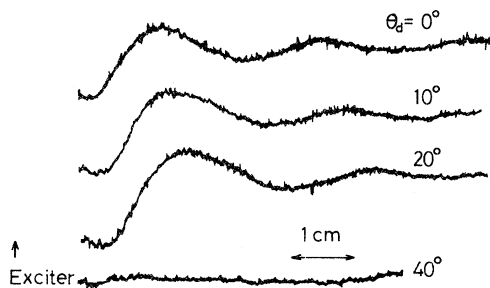


FIG. 3. Typical patterns of ion waves propagating along $\theta = 0^\circ$ and oblique to the magnetic field. The angle θ_d indicates that with respect to the magnetic field. $\omega/\omega_{ci} \approx 0.7$, $f = 350$ kHz, $f_{ci} \approx 5 \times 10^5$ sec $^{-1}$, $\omega_{pi}^2 \gg \omega_{ci}^2$.

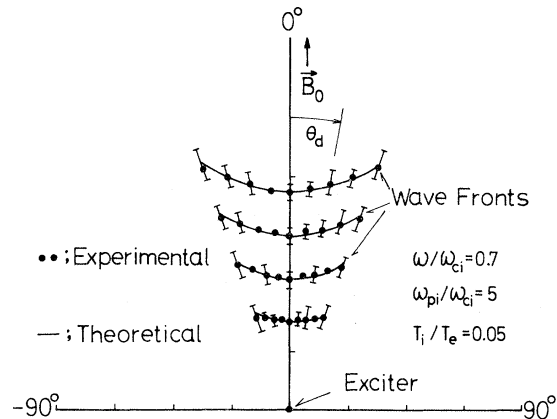


FIG. 4. Experimental and theoretical wave fronts (equivalent phase surfaces) of ion waves in a magnetized plasma. $\omega/\omega_{ci} \approx 0.7$, $\omega_{pi}/\omega_{ci} = 5$, $T_i/T_e \approx 0.05$. These are plotted in polar coordinates.

tained from the experimental data of Fig. 3, are plotted in terms of coordinates, where the angle is chosen as the detection angle. Those wave fronts mean equiphase surfaces. The observed wave fronts indicated typical properties in an anisotropic medium, which were not simple plane or spherical waves. (The theoretical wave fronts will be described later.) In Fig. 5, the observed phase velocities were indicated for various detection angles, where several exciting frequencies were chosen as parameters. The observed phase velocities for the radial direction are found to become faster with increasing detection angle and in increasing ratio of the frequency to the ion cyclotron frequency, ω/ω_{ci} .

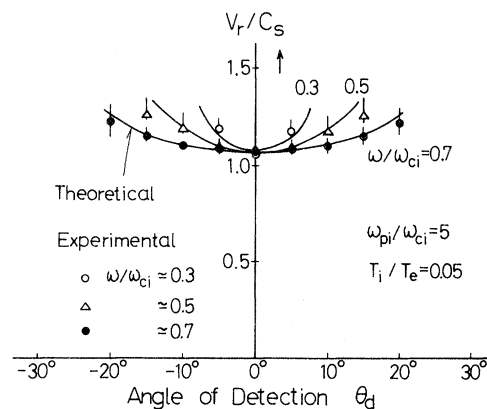


FIG. 5. Experimental and theoretical ray velocities versus the angle of detection for several values of ω/ω_{ci} . $\omega_{pi}/\omega_{ci} = 5$, $T_i/T_e \approx 0.05$.

IV. DISCUSSIONS

A. Comparison of observed phase velocities with theoretical ray velocities

In order to explain the experimental results in Sec. III, we must consider the wave characteristics in an anisotropic medium, i.e., in the magnetized plasma, which was described in the theoretical background in Sec. II. In a concept of the wave propagation in the anisotropic medium, it is important that the radial direction for the detection is the direction of the group velocity and is not that of the wave propagation in a phase-velocity surface. Although the simplest acoustic velocity of $T_i=0$ was investigated in Sec. II, we must consider the effect of ion temperature in order to explain the experimental results because of the finite ion temperature. For the effect of the ion temperature, the kinetic dispersion relation which is given Eq. (2), must be treated instead of Eq. (3). By using the kinetic dielectric constant, we can obtain numerically the angular dependence of the phase, group, and ray velocities, which were indicated in Fig. 6 for typical parameter values. In Fig. 6, those velocities are drawn for all direction with respect to the exciter, while the velocities were indicated only for one quarter region in Fig. 1. Although those velocities are similar to the cases of fluid model, there is a region of angle in Fig. 6,

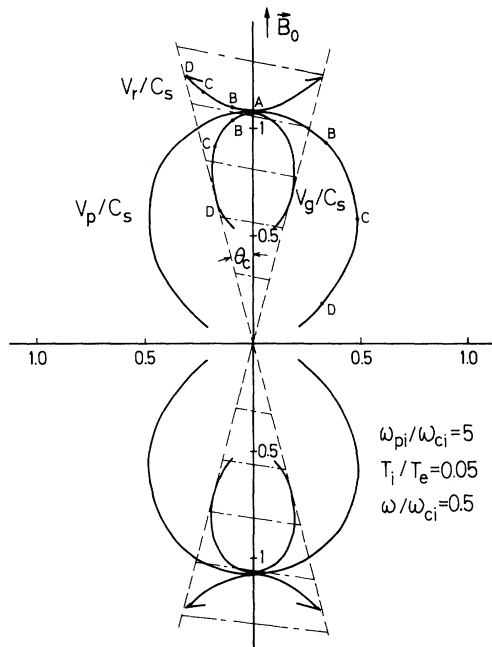


FIG. 6. Normalized phase velocity V_p , group velocity V_g , and ray velocity V_r in polar coordinates derived from a kinetic theory. In the shaded region, wave energy flows out from the exciter.

in which two values of group velocity coexist for a fixed angle. Of these parameter values, one value beyond the point D may not be observed because the mode is highly damped in comparison with another value. The difference between the kinetic and fluid treatment will become more clear in Fig. 7.

By the calculation of the ray velocities in the kinetic model for the experimental plasma parameter values, we obtained the theoretical results in Fig. 5. Those theoretical ray velocities were found to be nearly in accord with the observed phase velocities. By these ray velocities, the theoretical wave fronts, i.e., equiphase surfaces, could be obtained as theoretical lines indicated in Fig. 4. Those theoretical wave fronts were also shown to agree with the experimental results. In the results of Figs. 4 and 5, the phase velocities detected in radial directions were found to be explained by the theoretical ray velocities V_r .

Now, we consider the effect of the electron-neutral collision frequency ν_{en} which is of the same order as the applied frequency. In order to investigate the collisional effects, we derived the dispersion relation which includes the collisions. As the present experimental conditions satisfy $\omega_{ce}^2 \gg |\omega + i\nu_{en}|^2$ (ω_{ce} is the electron cyclotron frequency), we know that the effect of the electron-neutral collisions is neglected for the conditions of $|\omega$

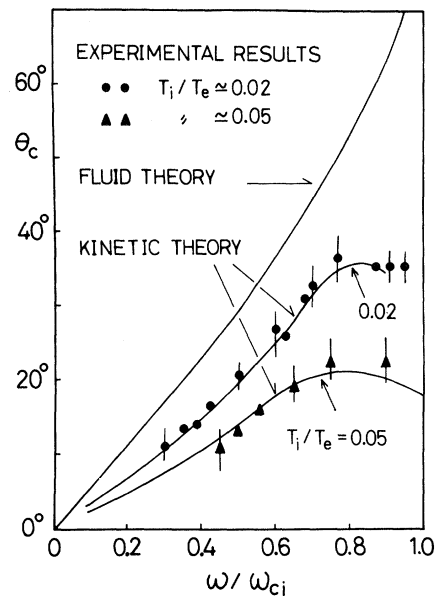


FIG. 7. Observed and theoretical cone angles for low-frequency regions. The theoretical results from fluid and kinetic theories are indicated by solid lines; experimental results are plotted as closed circles and triangles. The experimental conditions are $f = 100\text{--}400$ kHz, $f_{ci} \approx 400\text{--}500$ kHz, $T_i/T_e = 0.02\text{--}0.05$, $\omega_{pi}^2 \gg \omega_{ci}^2$.

$+i\omega_{en})\omega| \ll k_{\parallel}^2 C_e^2$ (C_e , the electron thermal velocity). The condition was usually satisfied in present experimental conditions except at $\theta=90^\circ$. That is, the effect of the electron-neutral collisions is negligible for present experiments. Furthermore, the effect of a plasma flow is small in present experimental conditions. Although the oblique detection of ion waves near the ion cyclotron frequency was reported by Hirose *et al.* (Ref. 5), they did not observe the ray velocities, which are the main results of present paper.

B. Relation of the experimental results to low-frequency resonance cones

When we consider an oscillating point source for low-frequency regions in a magnetized plasma, the low-frequency resonance cone,^{9,10} which had been reported in Ref. 11, must be considered. The cone angle θ_c for zero ion temperature in a fluid model was given by the following relation¹⁰:

$$\sin\theta_c = \frac{\omega}{\omega_{ci}} \left(1 + \frac{\omega_{ci}^2}{\omega_{pi}^2} - \frac{\omega^2}{\omega_{pi}^2} \right)^{1/2}. \quad (7)$$

The cone angle θ_c corresponds to the edge angle of the group-velocity surface in Fig. 2. In Fig. 6 of the kinetic treatment, the cone angle is also indicated as an edge cone angle of the group-velocity surface. Inside the cone angle, the group velocity can exist, i.e., the wave energy flows out from the exciter inside the cone angle. As the ray velocities observed in this paper correspond directly to the group velocity, the edge angle inside which wave signals (i.e., ray velocities) can be observed corresponds to the low-frequency resonance cone angle θ_c . The edge angle observed experimentally was plotted in Fig. 7.¹¹ The experimental data were plotted for the cases of $T_i/T_e \approx 0.02$ and 0.05. The

ion temperature was measured with a Faraday cup, which has three electrodes (two meshes and one plate collector). The theoretical cone angle of a fluid model was derived from Eq. (7). The kinetic cone angle was obtained from the edge angle of the group-velocity surface as Fig. 6. Several ratio of the ion temperature to the electron temperature were chosen. The cone angle are shown to be very sensitive to the temperature ratio. Those experimental results are nearly in accord with the kinetic cone angles. That is, the ray velocities observed in these experiments were found to be restricted inside the low-frequency cone angle. Figure 7 indicates that the finite-ion-temperature effects are important in the exact determination of the cone angles. The fact is physically explained as follows. The cone angle is determined by oblique propagations of ion waves as described above. Because the propagation characteristics, i.e., the phase velocity and the damping rate, of the oblique ion waves relate directly to the ion temperature, the cone angle is also affected by the ion temperature.

V. CONCLUSIONS

For an excitation by a small probe in a magnetized plasma, we could observe ray velocities (phase velocities in the direction of group velocities) of ion waves near the ion cyclotron frequency. This observation is a typical, important property of an anisotropic medium such as magnetized plasmas. The ray velocities, where the wave energy flowed out from the exciter, were found to be restricted inside a fixed cone angle which corresponds to low-frequency resonance cone angle.

¹K. N. Stepanov, Zh. Eksp. Teor. Fiz. **35**, 1150 (1958) [Sov. Phys.-JETP **8**, 808 (1959)].

²T. H. Stix, *Theory of Plasma Waves* (McGraw-Hill, New York, 1962), p. 225 and Chap. 3.

³D. D. Lominadze and K. N. Stepanov, Zh. Tekh. Fiz. **34**, 1823 (1964) [Sov. Phys.-Tech. Phys. **9**, 1408 (1965)].

⁴J. P. M. Schmidt, Phys. Rev. Lett. **31**, 982 (1972).

⁵T. Ohnuma, S. Miyake, T. Watanabe, T. Watari, and T. Sato, Phys. Rev. Lett. **30**, 535 (1973).

⁶A. Hirose, I. Alexeff, and W. D. Jones, Phys. Fluids

13, 2039 (1970); T. Ohnuma, S. Miyake, T. Sato, and T. Watari, Phys. Rev. Lett. **26**, 541 (1971).

⁷H. H. Kuehl, Phys. Fluids **16**, 1311 (1973).

⁸B. D. Fried and S. D. Conte, *The Plasma Dispersion Function* (Academic, New York, 1961).

⁹R. K. Fisher and R. W. Gould, Phys. Fluids, **14**, 857 (1971).

¹⁰H. H. Kuehl, Phys. Fluids **17**, 1636 (1974).

¹¹Observation of the resonance cone has been reported by T. Ohnuma, T. Kuwabara, K. Shibata, and S. Adachi [Phys. Rev. Lett. **37**, 206 (1976)].